Effects of temperature on surface modification of W exposed to He particles

C. Li[1], H. Greuner[2], Y.Yuan[3], G.N. Luo[4], B. Böswirth[2], B.Q. Fu[1], H.Y. Xu[1], Y.Z. Jia[1], W.Liu[1,*]

[1] Laboratory of Advanced Materials, School of Material Science and Engineering, Tsinghua University, Beijing 100084, China
[2] Max-Planck-Institut für Plasmaphysik, Boltzmannstr. 2, 85748 Garching, Germany
[3] School of Physics and Nuclear Energy Engineering, Beihang University, Beijing 100191, China
[4] Institute of Plasma Physics, Chinese Academy of Sciences, Hefei, Anhui 230031, China

Abstract

The effect of combined heating and helium particle flux on annealed tungsten samples has been studied in the neutral beam facility GLADIS. He beams with power densities of 2.4 MW/m^2 and 9.5 MW/m^2 were used to adiabatically load the samples to peak surface temperatures from ~ 950 °C (1223 K) to ~ 2700 °C (2973 K). Changes in the surface morphology resulting from combined heat and the flux exposure were studied for He fluences up to 3×10^{22}/m^2. Typical structures for the sample loaded at ~ 950 °C (1223 K) were blisters with a clear grain orientation dependence and the largest blisters formed on grains with <001> surface normal. However at higher temperatures, blistering was more easily suppressed for grains near this orientation because the growth of larger blister takes place more slowly. An evolution from a “porous structure” to a “coral-like structure” with increasing fluence was observed on the samples loaded at the highest temperature. Based on these results mechanisms for surface modification at different temperatures are discussed and a texture with <001> parallel to the normal direction of the grains is suggested to optimize the plasma facing material due to their stronger resistance to early stage blistering.

Key words: W; He; high heat flux; grain orientation

* Corresponding author. Tel.: +86 10 62772852; fax: +86 10 62771160

E-mail address: liuw@mail.tsinghua.edu.cn

1. Introduction

Tungsten (W) is a promising candidate for future use in fusion reactors as a plasma facing material, due to its high melting point, high thermal conductivity, low tritium inventory and other favorable characteristics [1,2]. During such usage it will be exposed to both particle irradiation and high heat flux loads. Particle irradiation from the fusion plasma, especially helium (He) bombardment, is expected to lead to performance degradation of W components due to the development of significant changes in surface morphology, such as the formation of blisters, holes, fiber-form nanostructures and coral-like structures [2-7]. In addition, synergistic effects between heat loading and particle irradiation can accelerate such surface damage [2]. The performance of W under the combined action of both heat and a particle flux has therefore been studied keenly in recent years [2,5]. In fusion devices during steady-state heat flux conditions active cooling of the plasma facing components ensures that the surface temperature is kept at a relatively low level. However, during transient phenomena such as vertical displacement events (VDEs), a high amount of energy can be deposited in a short period leading to a large increase in temperature. The He-induced surface damage behavior of W over a range of different temperatures is therefore a serious concern.

Previous studies have reported that the extent and nature of He-induced surface damage are not only affected by the He fluence, but also greatly influenced by temperature [2,6,8]. The schematic shown in Fig. 1 summarizes the results reported in Ref. [2], [5] and [7], and shows the observed relationship between surface modification, fluence and peak surface temperature. The mechanism for the formation of these surface morphologies is, however, not fully understood, especially the effects of temperature dependence. In addition, some studies have found an orientation dependence for He-induced damage [3,5,8]. This is interesting as it may provide a way to optimize the plasma facing material by control of the crystallographic texture.

Based on the previous work the present study has been carried out to investigate the influence of both temperature and orientation on surface modification of W under exposure to high heat and He fluxes. In particular the investigation focuses on the combined effects of high heat flux (HHF) loading and He irradiation, and the relationship with damage behaviors at different temperatures.

2. Experimental

The W material used in this study was made by AT&M, China (>99.9% purity, sintered and warm-rolled). The as-received material was recrystallized at 1400 °C (1673 K) under argon gas, resulting in an average grain size of ~24 μm. Samples for investigation of surface damage were cut with dimensions of 12×10×3 mm^3. The samples were mechanically polished on top surface to a mirror finish before loading. A scanning electron microscope (SEM) image showing a sample surface before loading is shown in Fig. 2.

He-flux/heating experiments were performed using the neutral beam HHF test facility GLADIS [7,9] at IPP Garching, Germany. The He beam in this facility generates homogeneous heating due to the nearly complete absorption of the beam power on the W surface [9]. Although the sample holder is water cooled, due to poor thermal contact cooling of the W after each pulse is assumed to take place mainly by thermal radiation [1]. Surface temperatures were measured with pyrometers and with an IR camera. Further details about the

surface temperature measurements can be found in Ref. [1]. An example plot of surface temperature *vs.* time for 5 s heating is shown in Fig. 3. In this work, different peak surface temperatures were investigated by controlling the pulse length. A similar total incident fluence was applied in each of the experimental campaigns. The interval between consecutive pulses was taken as 15 min, to ensure a start temperature below 300 °C (573 K).

Experiments were carried out using two different power densities. In the case of 2.4 MW/m^2 loading, the corresponding He flux was 7×10^{20} m^{-2}s^{-1} with a particle energy of 22 keV. For the 9.5 MW/m^2 loading the He flux was 2×10^{21} m^{-2}s^{-1} with a particle energy of 36 keV. The main experimental data are summarized in Table 1. The He-induced surface modifications were analyzed with the aid of scanning electron microscopy, focused ion beam (FIB) milling and electron backscattered diffraction (EBSD) imaging.

3. Results

3.1. He-loading at a low surface temperature (T_{peak} ~950 °C /1223 K)

Many blisters were found on the surface of the low temperature loaded sample (sample LT), with many ruptured to form lids and grooves. Fig. 4a shows typical microstructures where it is seen that the extent of blistering varying greatly from grain to grain.. The blisters parameters, such as size, frequency and shape, also differ from one grain to another. Circular blisters are found in grains A and B, both of which are partly ruptured. The blisters in grain B show however more rupturing than those in grain A. In grain C, larger blisters are observed, with a size in the range > 1~2 μm, whereas in grains A and B the blisters are about 1 μm or less. In addition many ruptured blisters in grain C are characterized by irregular shapes due to the coalescence of several circular blisters. Figures 4b and 4c show images of ruptured large and small blisters, in grains C and B, respectively.

For all ruptured blisters, most of them retain their lids, which are about 30~50 nm thick. Blister rupturing is observed to take place at the blister periphery, resulting in formation of a groove with rough planar base.

Based on the observation of a strong grain to grain variation in blistering, EBSD was used to compare the behavior with grain orientation. The results of the EBSD measurements confirmed a clear correlation between blistering and grain orientation. A total of 49 grains with similar surface features in grains A, B and C were investigated. The surface orientations (normal direction [ND]) of these grains are shown in inverse pole figure format in Fig. 4d. The degree of blistering in these grains is indicated by different symbols: solid squares indicate “light” blistering (beginning of blister formation, as in grain A), crosses indicate “medium” blistering (small blisters, as in grain B), and hollow circles indicate “heavy” blistering (large blisters, as in grain C).

It is evident from Fig. 4d that large blisters only appeared in grains with near <001> surface normal, and that grains with a near-<111> surface suffered the least damage. Medium degree blistering occurred in grains with a near-<011> surface and in grains with surface orientations between <001> and <111> .

3.2. He-loading at an intermediate surface temperature (T_{peak} ~1900 °C /2173 K)

The intermediate temperature loaded sample (sample MT) was tested under similar loading conditions as sample LT, except that the pulse length was changed to 5 s to achieve a

higher peak surface temperature of about 1900 °C (2173 K). An example of a typical loaded surface microstructure is shown in Fig. 5a. The grains show different features to those observed in the LT sample. The morphology of the observed features also varies significantly from grain to grain. The features are classified into three types: porous/coral-like structures without grooves (as in grain D), coral-like structures with small grooves (as in grain E) and porous structures with large grooves and occasional lids and blisters (as in grain F), as shown in Figures 5b-d. Compared with Fig. 4, the grooves seen in grains E and F share a similar shape and distribution with the blisters seen in grains B and C, respectively. In total 52 grains were investigated by EBSD to examine the orientation dependence of the surface morphology. The results are shown in Fig. 5e. The orientation of grains with surface structures similar to those of grains D, E and F are labeled with hollow circles, solid squares and crosses respectively. It is evident from the inverse pole figure that the small grooves with a diameter of about 1μm were formed in grains with surface orientation away from <001>. Although structures without grooves and structures with large grooves were both found for near <001> grains, the proportion of the large grooves was very small. These observations will be discussed in detail in Section 4.

3.3. He-loading at a high surface temperature (T_{peak} ~2700 °C /2973 K)

Three samples were examined under high temperature loading, as shown in Table 1. Sample HT and sample HT-8 were both exposed to a similar incident fluence as samples LT and MT, at peak surface temperatures of approx. 2700 °C (2973 K) (still below the melting point ~3410 °C (3683 K) [11]). Typical “coral-like” structures were observed on both surfaces with no obvious orientation dependence, as shown in Fig. 6. The third sample, HT-1, was exposed to a lower total fluence of $3.70\times10^{21}/m^2$ at a similar temperature. In this sample a porous structure was developed, including pinholes (several nanometers in diameter) and holes (several hundred nanometers in diameter), and the hole density varies in certain extent from grain to another, as shown in Fig. 7.

FIB cross-sections prepared from samples HT-1 and HT-8 in Fig. 7c and 6c show that the depth of the damage layer increased from ~400 nm to ~1 μm with the increase of fluence. This evolution from a “porous structure” to a “coral-like structure” with increasing fluence is discussed in detail in the following section.

4. Discussion

In studies of energetic He injection into W, blistering has been frequently reported [2,4,5]. Blisters and ruptured blisters of morphology similar to those seen in sample LT (Fig. 4) have been found in many previous studies, not only on W surfaces, but also on other metal surfaces, such as Nb, V and Mo [3]. A number of different models have been put forward to describe and explain the formation of surface blisters on He-bombarded metal surfaces [3,12]. In our study, the thickness of some blister lids was measured, and found to be about 30~50nm, as seen in Fig. 4b. This thickness correlates well with the calculated projected range of 22 keV He in W, which is about 45 nm [10]. Additionally the ruptured blisters were found to have a rough planar base. These observations suggest a bubble coalescence and plastic deformation mechanism, which should be viewed as a kind of gas pressure model for blistering, as shown in Fig. 8a and explained in the following.

At the initial stage, He bubbles form at a depth close to the projected range for low temperatures [13], and then bubble coalescence will leads to the formation of penny-shaped cracks at this depth [12]. The results of ab initio calculations and molecular dynamics simulations [4,14] suggest that He_n and He_nV_m (He-vacancy) clusters are both likely to form. The diffusion energy barriers associated with such clusters in W are much higher than that for single He atom transport. Therefore, He_n and He_nV_m clusters form at the projected range, and then grow to form small bubbles during irradiation either by point defect accumulation or by punch out of interstitial dislocation loops. Once the bubble density is high enough and neighboring bubbles start to touch each other, coalescence of small bubbles takes place, leading to the formation of penny-shaped cracks parallel to the surface, which are unstable high pressure cavities, leading to the plastic deformation of the surface layer. [12] The cracks can spread parallel to the surface due to the stress field around crack tips, and the following deformation of the covering surface layer will form a blister. When the critical size of blisters reaches, rupturing at the periphery takes place, to form grooves either with or without lids. Fig. 8b is a high-magnification image of a blister and a groove, which shows that the above described morphology of the groove with rough planar base is in good agreement with the SEM observation. Both of the two deformation processes are influenced by many factors, such as the surface atom density [15] and mechanical properties [3,12]. These parameters vary with different crystal orientations, leading to the orientation dependence of blistering, which has also been observed on other material surfaces [3,5]. As early as the 1960s, Milacek and Daniels [15] argued that the blister density increases with the amount of retained gas, which is assumed to be highest for implantation along open directions (e. g. , <111> in a bcc lattice). According to our study, it is suggested, however that the increased implantation along open directions is only important at the very initial stage of exposure, before bubble coalescence takes place. Once the crack growth and deformation stage is reached, differences of mechanical properties along different directions have to be taken into consideration. A comprehensive and systematic interpretation is planned in our future work. It should be noted that the fine structures observed on the covers of blisters and in areas without blisters, as shown in Fig. 8b might be caused by physical sputtering.

At temperatures high enough to allow break up of the He_n and He_nV_m clusters (as pointed out in Ref. [7] a peak surface temperature of 2100 °C (2373 K) is sufficient to break up 1 eV He–He bonds), He can diffuse deeper into the W bulk. The mechanism for evolution of surface morphology is therefore modified as shown in Fig. 9. Compared with the low-temperature evolution process, the major difference is that He_n and He_nV_m clusters form over a much wider distribution of depths. Individual clusters still grow and link up, resulting in the formation of many bubbles/holes of various sizes in near-surface regions, and hence a porous structure. The SEM observations of sample HT-1 (Fig. 7) confirms the predicted morphology of this stage. Subsurface He-bubbles have been observed with transmission electron microscopy by other researchers[16,17]. In addition, it is seen from Fig. 7 that hole density varies in certain extent from grain to gain. This observation might be caused by the different incident fluence and diffusion process of He atoms due to different surface atoms density depending on grain orientations. Relative orientation analysis is of interest for our future work. With increasing fluence, the bubbles/holes develop into a coral-like structure, as observed on sample HT-8 (Fig. 6). The morphology differences between different grains

become less significant as a result of the higher fluence. This process will be influenced by temperatures since it is diffusion-controlled. It can be noted also that as shown in Fig. 6c, the depth of these structures is much larger than the depth of sputtering (Table 1). Erosion by sputtering therefore contributes only a minor part during the evolution of such structures.

For samples loaded with low He fluence (see Table 1) at an intermediate temperature, in contrast to other reported results where a high fluence was used [2], the typical structure was not a sputtering-induced wavy structure, but rather one with grooves and holes. The variation of groove formation with different surface orientation corresponds well to the pattern seen for blistering in low temperature samples, in such aspects as size, shape and distribution. It is considered therefore that the final microstructure after He-loading is dependent on a competitive relationship between two processes: the formation of blisters, and the evolution of a “coral-like structure”, acting as the main process at low and high temperatures, respectively. For intermediate temperatures, both processes can occur, and a variety of mixed structures can be formed, such as blisters/grooves with holes. The observation of different structures in near <001> grains can be explained assuming that the blister growth takes place more slowly in grains of this orientation. Therefore in most near <001> grains the formation of holes occurs before blistering, resulting in simple porous/coral-like structures, whereas in grains with other orientation, blisters had formed and ruptured before the formation of holes, resulting in mixed structures.

The surface temperature of actual water-cooled divertor components is relatively low, typically ~1000 °C (1273 K). Under these conditions He-induced surface damage similar to that of sample LT (blistering) can be expected. For loading with a mixture of H and He, the He component will dominate the evolution of the surface morphology [18]. The He fraction of the particle bombardment in a fusion divertor is very nevertheless low (just 5–10 %). Therefore, it is reasonable to infer that under actual working conditions, W surface damage will be in the early stage of blistering, which has been confirmed by our latest study.. In such a case grains with near-<001> surface, where the deformation-induced blister formation takes longer, may have stronger resistance to blistering than other orientations. Hence, it is suggested that a texture with <001> parallel to the normal direction of the grains will be beneficial in order to optimize the plasma facing material.

5. Conclusion

The changes in surface morphology of annealed W samples adiabatically loaded by a high energy He flux at different temperatures have been studied. The results suggest that the final microstructure is dependent on a competitive relationship between two processes. One is the formation of blisters, which is the main process at a low temperature and shows a clear orientation dependence. The largest blisters were formed in grains with a near <001> surface normal. The other process is the evolution from a “porous structure” to a “coral-like structure”, which is diffusion-controlled, and influenced by temperature. At a sufficiently high temperature, this process dominates the damage process. At intermediate temperatures, both processes occur, resulting in a variety of mixed microstructures.

The surface modifications, whether formation of blisters or coral-like structures, will influence thermal properties, mechanical properties and tritium retention of W, and may lead to plasma contamination. However, the relative strength of the two processes can be

controlled by adjusting the grain orientation with consideration of the service temperature. Surface damage might be reduced therefore by finding an optimal solution. According to the present study, W surface damage under actual working conditions is expected to be in the early stage of blistering, the development of near <001> surface grains is therefore suggested due to their stronger resistance to early stage blistering.

Acknowledgements

The authors gratefully acknowledge Dr. Xiaochun Li, Dr. Hans Maier and Dr. Armin Manhard for their valuable discussions, Gabriele Matern and Dandan Zhang for their assistance in SEM and EBSD investigations , and would like to thank Ms. Petra Douglas for other help in this work. Special thanks to Dr. Andy Godfrey for his suggestions on the manuscript.

This work was supported by National Magnetic Confinement Fusion Science Program of China under Grant 2013GB109004，2011GB110003 and 2013GB105001 and the National Nature Science Foundation of China under Contract Nos. 51071095 and 50971077, and the Joint Sino-German research project GZ 763, and the Tsinghua Scholarship for Overseas Graduate Studies.

References

[1] Y. Yuan, H. Greuner, B. Böswirth, et al., J. Nucl. Mater., 433 (2013) 523.

[2] K. Tokunaga, S. Tamura, N. Yoshida, et al., J. Nucl. Mater., 329–333 (2004) 757.

[3] B.M.U. Scherzer, Development of surface topography due to gas ion implantation, in: R. Behrisch (Ed.), Sputtering by Particle Bombardment, Springer-Verlag, Berlin, 1981, pp. 271-355.

[4] X.C. Li, X.L. Shu, Y.N. Liu, et al., J. Nucl. Mater., 426 (2012) 31.

[5] Y. Yuan, H. Greuner, B. Böswirth, et al., J. Nucl. Mater., 437 (2013) 297.

[6] S. Kajita, W. Sakaguchi, N. Ohno, et al., Nucl. Fusion, 49(2009) 095005.

[7] H. Greuner, H. Maier, M. Balden, et al., J. Nucl. Mater., 417 (2011) 495.

[8] S.J. Zenobia, L.M. Garrison, G.L. Kulcinski, J. Nucl. Mater., 425 (2012) 83.

[9] H. Greuner, B. Böswirth, J. Boscary, et al., J. Nucl. Mater., 367–370 (2007) 1444.

[10] M. J. Berger, Stopping-Power and Range Tables for Electrons, Protons, and Helium Ions, http://www.nist.gov/pml/data/star/index.cfm

[11] Y. Yuan, H. Greuner, B. Böswirth, et al., J. Nucl. Mater., 438 (2013) S229.

[12] M. Kaminsky, S.K. Das, Radiation Blistering–Recent Developments, IX Summer School and Symposium on the Physics of Ionized Gases, Dubrovnik, Yugoslavia, August 28–September 2, 1978.

[13] K.O.E. Henriksson, K. Nordlund, A. Krasheninnikov, et al., Fusion Sci. Technol., 50 (2006) 43.

[14] C.S. Becquart, Phys. Rev. Lett., 97 (2006) 196402.

[15] L.H. Milacek, R.D. Daniels, J.A. Cooley, J. Appl. Phys., 39 (1968) 2803.

[16] M. Yamagiwa, S. Kajita, N. Ohno, et al., J. Nucl. Mater., 417 (2011) 499.

[17] S. Kajita, N. Yoshida, R. Yoshihara, et al., J. Nucl. Mater., 418 (2011) 152.

[18] H. Greuner, H. Maier, M. Balden, et al., J. Nucl. Mater., 442 (2013) S256.

Figures and Table

Sample label	Peak surface temperature [°C/K]	Pulse length [s]	No. of pulses	Incident fluence [m^{-2}]	Calculated penetration depth [nm]	Calculated physical sputtering [nm]
LT	~950/1223	1.6	27	3×10^{22}	45	~20
MT	~1900/2173	5	8	3×10^{22}	45	~20
HT	~2720/2993	11	4	3×10^{22}	45	~20
HT-8	~2680/2953	2.3	8	3×10^{22}	73	~15
HT-1	~2680/2953	2.2	1	4×10^{21}	73	~2

Table 1. The main loading parameters for the five investigated W samples. The penetration depth was calculated according to Ref. [10].

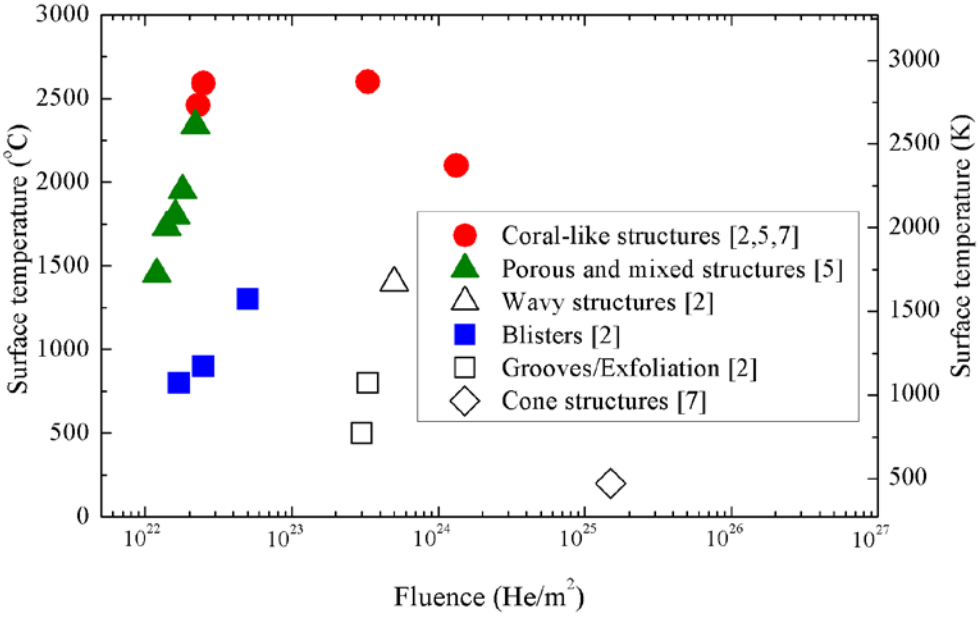

Fig. 1. Schematic of the relationship between surface modification, fluence and peak surface temperature [2,5,7].

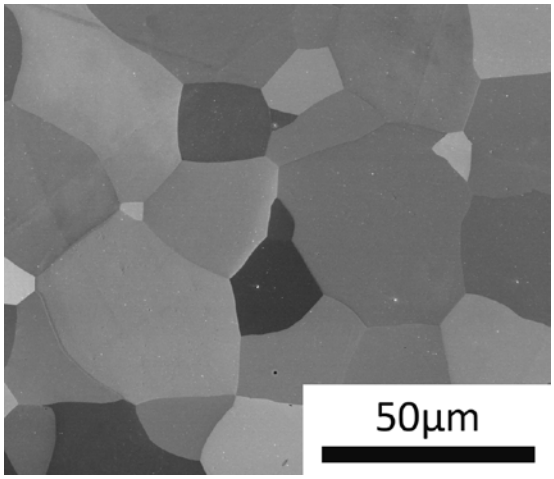

Fig. 2. SEM image of the original polished W surface.

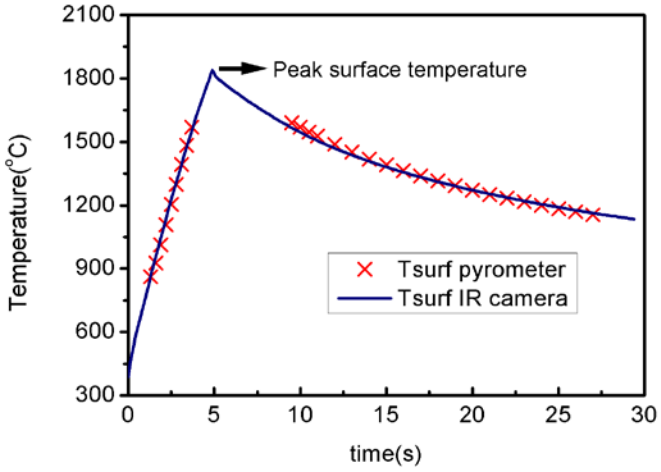

Fig. 3. Surface temperature evolution of the 2.4 MW/m^2 loaded sample during the 5 s heat loading.

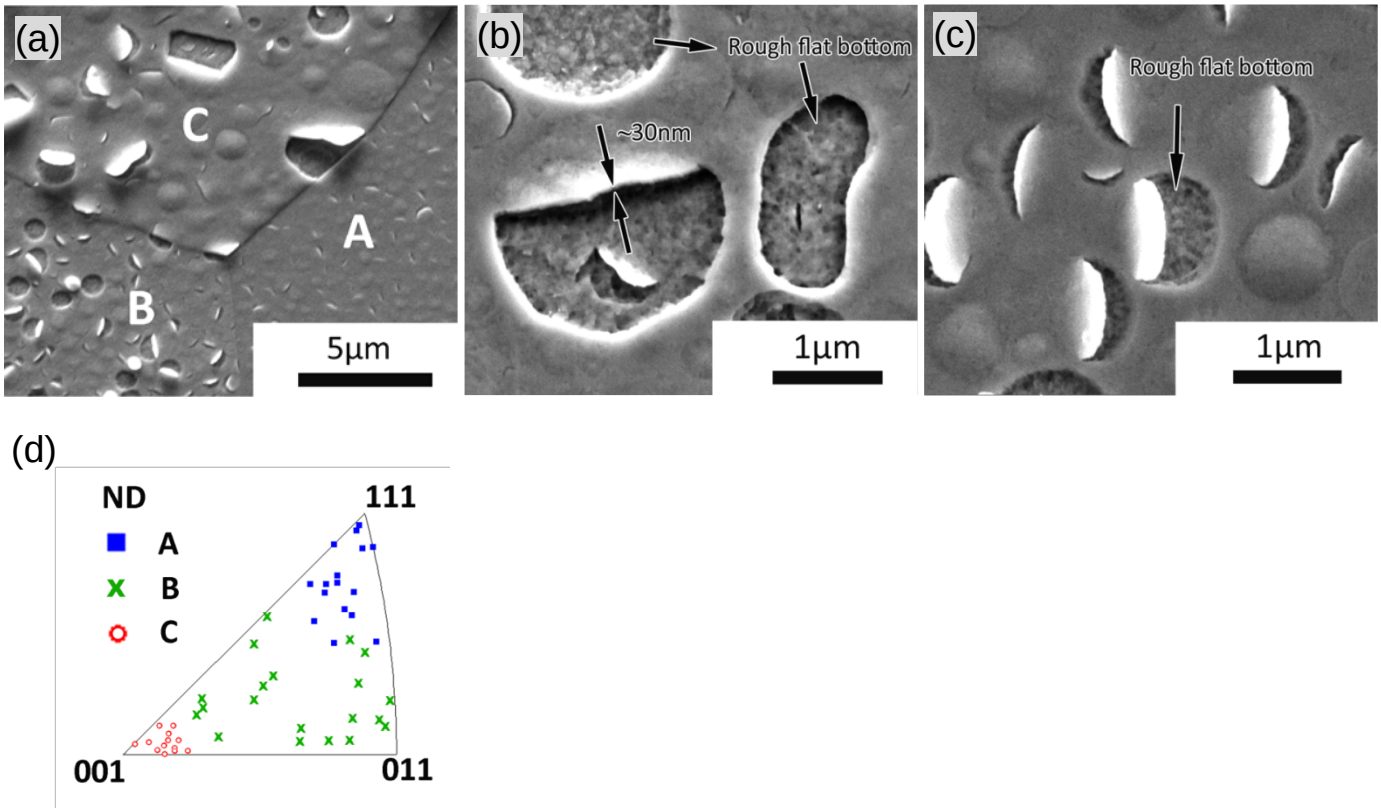

Fig. 4. (a) Surface morphology of the W surface loaded with repeated He pulses at the peak temperature of about 950 °C (1223K) and He fluence of $2.93\times10^{22}/m^2$ (sample LT). (b-c) Magnification of ruptured large blisters (as grain C) and ruptured small blisters (as grain A and B), respectively. (d) Inverse pole figure of the normal direction [ND] of the grain surface with respect to the cubic axes of the grains. The grains with different degrees of blistering are indicated by different symbols.

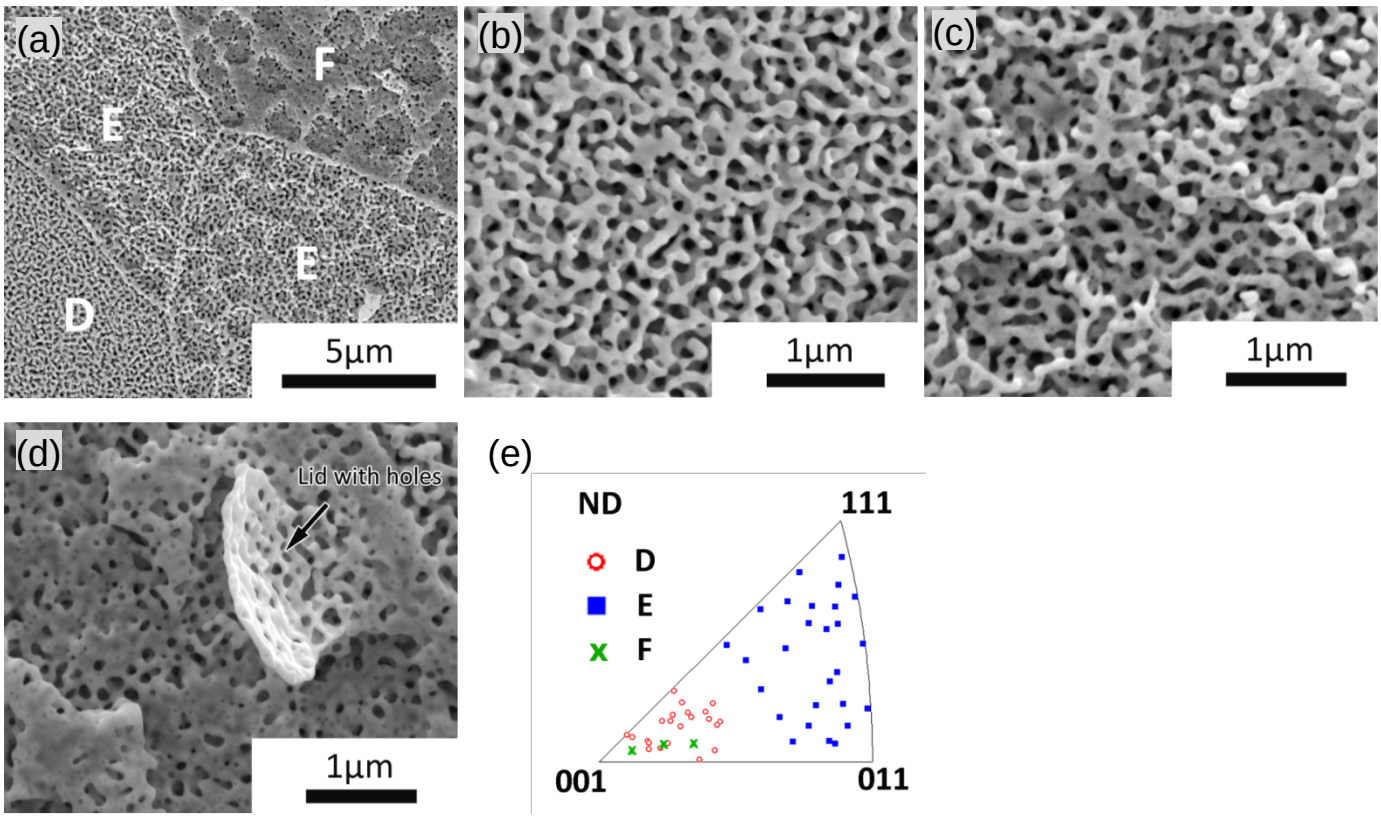

Fig. 5. (a) Surface morphology of the W surface loaded with repeated He pulses at the peak temperature of about 1900 °C (2173K) and He fluence of $2.74\times10^{22}/m^2$ (sample MT). (b-d) Magnification of porous/coral-like structure without grooves (as grain D), coral-like structure with small grooves (as grain E) and porous structure with large grooves (as grain F), respectively. (e) Inverse pole figure of the normal direction [ND] of the grain surface with respect to the cubic axes of the grains. The surface morphology on the grains is classified into without and with small/large grooves, which are indicated by different symbols.

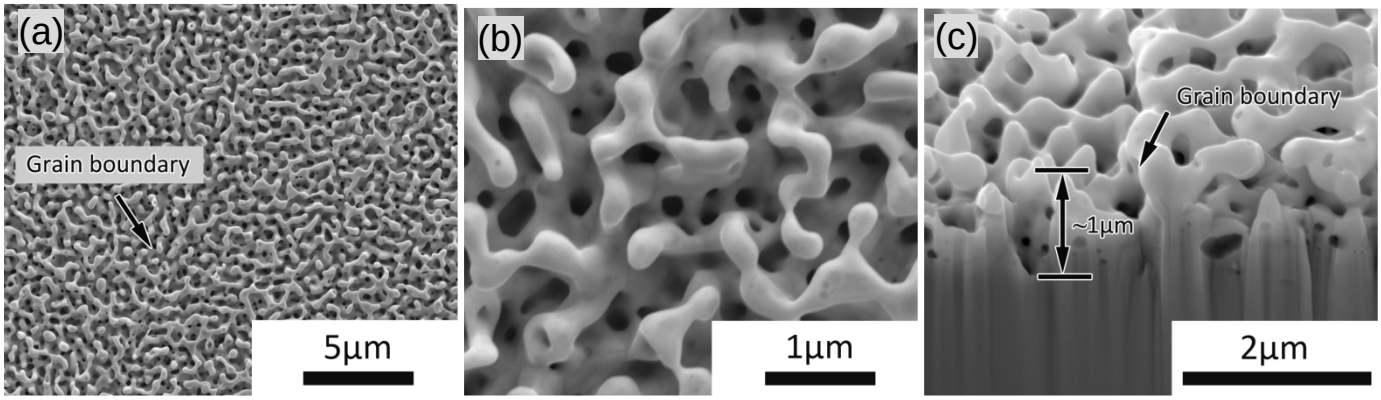

Fig. 6. Surface morphology of the W surface loaded with repeated He pulses at the peak temperature of about 2680 °C (2953K) and He fluence of $3.04\times10^{22}/m^2$ (sample HT-8). (a) Top view. (b) Magnification. (c) FIB cross section.

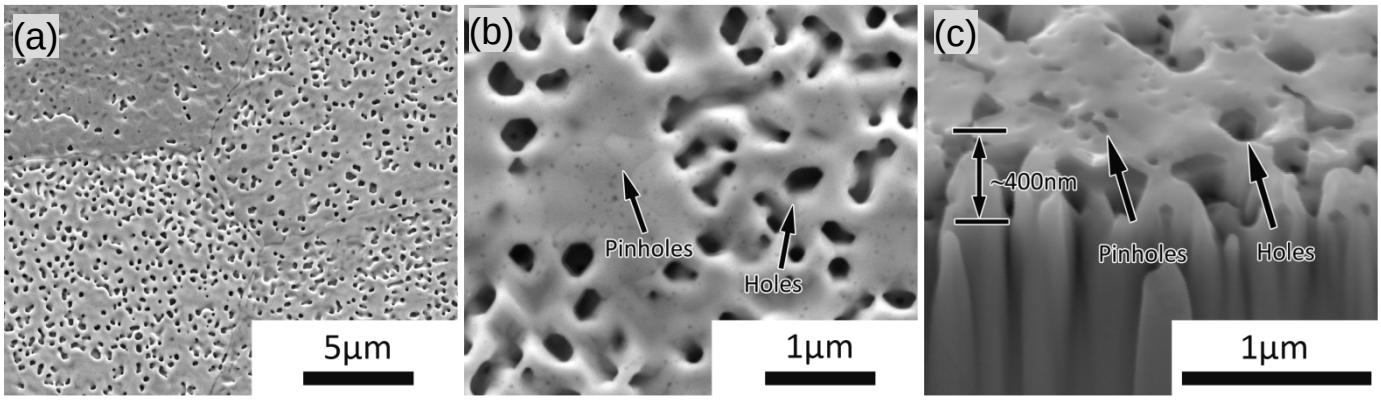

Fig.7. Surface morphology of the W surface loaded with repeated He pulses at the peak temperature of about 2680 °C (2953K) and He fluence of $3.70\times10^{21}/m^2$ (sample HT-1). (a) Top view. (b) Magnification. (c) FIB cross section.

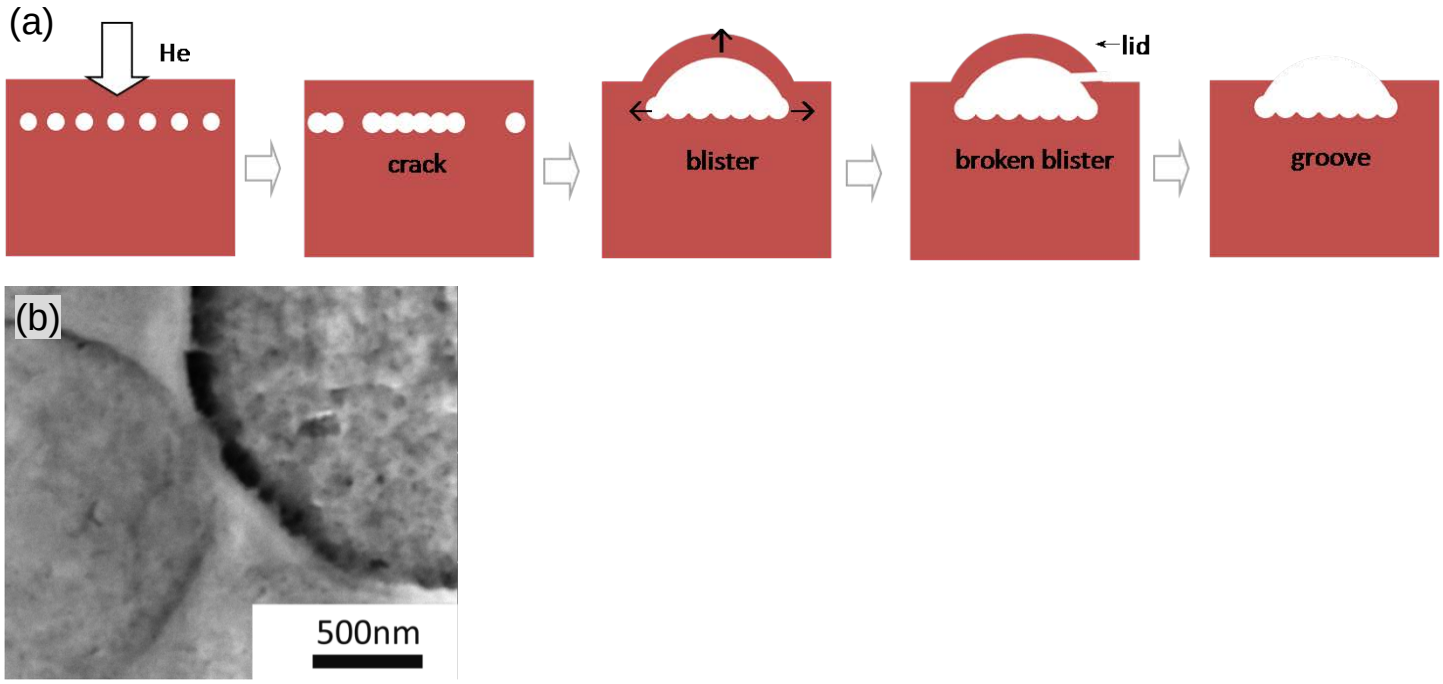

Fig.8. (a) The schematic diagrams of bubble coalescence and plastic deformation model of blister formation.

(b) Magnification of a blister and a groove on sample LT.

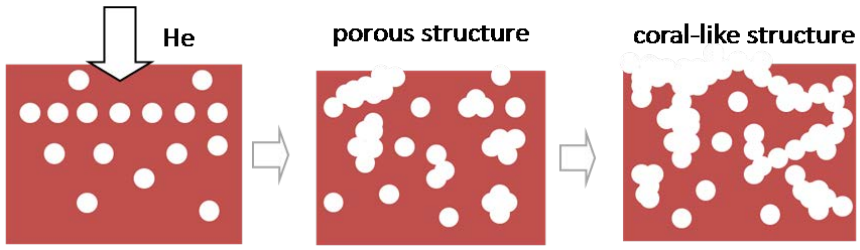

Fig.9. The schematic diagrams of the evolution to a "coral-like structure".